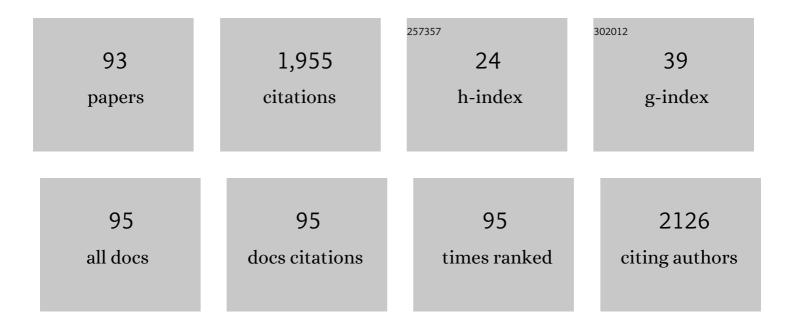
List of Publications by Year in descending order

Source: https://exaly.com/author-pdf/531809/publications.pdf Version: 2024-02-01



FELLY HOEMANN

#	Article	IF	CITATIONS
1	Lattice swelling and modulus change in a helium-implanted tungsten alloy: X-ray micro-diffraction, surface acoustic wave measurements, and multiscale modelling. Acta Materialia, 2015, 89, 352-363.	3.8	123
2	3D lattice distortions and defect structures in ion-implanted nano-crystals. Scientific Reports, 2017, 7, 45993.	1.6	96
3	Consistent determination of geometrically necessary dislocation density from simulations and experiments. International Journal of Plasticity, 2018, 109, 18-42.	4.1	94
4	Non-Contact Measurement of Thermal Diffusivity in Ion-Implanted Nuclear Materials. Scientific Reports, 2015, 5, 16042.	1.6	78
5	Measurements of stress fields near a grain boundary: Exploring blocked arrays of dislocations in 3D. Acta Materialia, 2015, 96, 229-236.	3.8	76
6	Residual stresses in Linear Friction Welding of aluminium alloys. Materials & Design, 2013, 50, 360-369.	5.1	60
7	Dislocation density distribution at slip band-grain boundary intersections. Acta Materialia, 2020, 182, 172-183.	3.8	60
8	Crack tip deformation fields and fatigue crack growth rates in Ti–6Al–4Vâ~†. International Journal of Fatigue, 2009, 31, 1771-1779.	2.8	50
9	Thermal diffusivity degradation and point defect density in self-ion implanted tungsten. Acta Materialia, 2020, 193, 270-279.	3.8	47
10	X-ray micro-beam characterization of lattice rotations and distortions due to an individual dislocation. Nature Communications, 2013, 4, 2774.	5.8	46
11	Strain tomography of polycrystalline zirconia dental prostheses by synchrotron X-ray diffraction. Acta Materialia, 2011, 59, 2501-2513.	3.8	42
12	Lifetime of sub-THz coherent acoustic phonons in a GaAs-AlAs superlattice. Applied Physics Letters, 2013, 102, .	1.5	41
13	Mapping the full lattice strain tensor of a single dislocation by high angular resolution transmission Kikuchi diffraction (HR-TKD). Scripta Materialia, 2019, 164, 36-41.	2.6	39
14	Evaluation of the overload effect on fatigue crack growth with the help of synchrotron XRD strain mapping. Engineering Fracture Mechanics, 2010, 77, 3216-3226.	2.0	38
15	Observation of Transient and Asymptotic Driven Structural States of Tungsten Exposed to Radiation. Physical Review Letters, 2020, 125, 225503.	2.9	38
16	Transient grating spectroscopy: An ultrarapid, nondestructive materials evaluation technique. MRS Bulletin, 2019, 44, 392-402.	1.7	37
17	The effect of helium implantation on the deformation behaviour of tungsten: X-ray micro-diffraction and nanoindentation. Scripta Materialia, 2018, 146, 335-339.	2.6	36
18	Effect of microstructures and texture development on tensile properties of Mg–10Gd–3Y alloy. Materials Science & Engineering A: Structural Materials: Properties, Microstructure and Processing, 2011, 528, 2250-2258.	2.6	34

#	Article	IF	CITATIONS
19	Residual stresses and microstructure in Powder Bed Direct Laser Deposition (PB DLD) samples. International Journal of Material Forming, 2015, 8, 245-254.	0.9	33
20	Nanoscale imaging of the full strain tensor of specific dislocations extracted from a bulk sample. Physical Review Materials, 2020, 4, .	0.9	32
21	Temperature dependence of helium-implantation-induced lattice swelling in polycrystalline tungsten: X-ray micro-diffraction and Eigenstrain modelling. Scripta Materialia, 2015, 107, 96-99.	2.6	30
22	Analysis of strain error sources in micro-beam Laue diffraction. Nuclear Instruments and Methods in Physics Research, Section A: Accelerators, Spectrometers, Detectors and Associated Equipment, 2011, 660, 130-137.	0.7	28
23	Glancing-incidence focussed ion beam milling: A coherent X-ray diffraction study of 3D nano-scale lattice strains and crystal defects. Acta Materialia, 2018, 154, 113-123.	3.8	28
24	Correcting for contact area changes in nanoindentation using surface acoustic waves. Scripta Materialia, 2017, 128, 83-86.	2.6	24
25	Micro-beam Laue alignment of multi-reflection Bragg coherent diffraction imaging measurements. Journal of Synchrotron Radiation, 2017, 24, 1048-1055.	1.0	24
26	Hardening and Strain Localisation in Helium-Ion-Implanted Tungsten. Scientific Reports, 2019, 9, 18354.	1.6	24
27	Modified deformation behaviour of self-ion irradiated tungsten: A combined nano-indentation, HR-EBSD and crystal plasticity study. International Journal of Plasticity, 2020, 135, 102817.	4.1	24
28	Laue-DIC: a new method for improved stress field measurements at the micrometer scale. Journal of Synchrotron Radiation, 2015, 22, 980-994.	1.0	23
29	<i>In</i> - <i>situ</i> high-temperature tensile testing of a polycrystalline nickel-based superalloy. Materials at High Temperatures, 2016, 33, 338-345.	0.5	23
30	Probing intra-granular deformation by micro-beam Laue diffraction. Procedia Engineering, 2009, 1, 193-196.	1.2	22
31	Helium-implantation-induced lattice strains and defects in tungsten probed by X-ray micro-diffraction. Materials and Design, 2018, 160, 1226-1237.	3.3	22
32	Imaging of grain-level orientation and strain in thicker metallic polycrystals by high energy transmission micro-beam Laue (HETL) diffraction techniques. International Journal of Materials Research, 2012, 103, 192-199.	0.1	22
33	High energy transmission micro-beam Laue synchrotron X-ray diffraction. Materials Letters, 2010, 64, 1302-1305.	1.3	21
34	Increase in elastic anisotropy of single crystal tungsten upon He-ion implantation measured with laser-generated surface acoustic waves. Applied Physics Letters, 2016, 109, .	1.5	21
35	Numerical exploration of the Dang Van high cycle fatigue criterion: application to gradient effects. Journal of Mechanics of Materials and Structures, 2009, 4, 293-308.	0.4	20
36	X-ray laser–induced electron dynamics observed by femtosecond diffraction from nanocrystals of Buckminsterfullerene. Science Advances, 2016, 2, e1601186.	4.7	20

#	Article	IF	CITATIONS
37	Nanoscale lattice strains in self-ion implanted tungsten. Acta Materialia, 2020, 195, 219-228.	3.8	20
38	Triaxial residual strains in a railway rail measured by neutron diffraction. Journal of Strain Analysis for Engineering Design, 2009, 44, 563-568.	1.0	19
39	Probing multi-scale mechanical damage in connective tissues using X-ray diffraction. Acta Biomaterialia, 2016, 45, 321-327.	4.1	19
40	Dislocation-based plasticity model and micro-beam Laue diffraction analysis of polycrystalline Ni foil: A forward prediction. Philosophical Magazine, 2010, 90, 3999-4011.	0.7	18
41	Polycrystal deformation analysis by high energy synchrotron X-ray diffraction on the I12 JEEP beamline at Diamond Light Source. Materials Letters, 2010, 64, 1724-1727.	1.3	16
42	Characterising Ion-Irradiated FeCr: Hardness, Thermal Diffusivity and Lattice Strain. Acta Materialia, 2020, 201, 535-546.	3.8	16
43	Mapping the dislocation sub-structure of deformed polycrystalline Ni by scanning microbeam diffraction topography. Scripta Materialia, 2011, 64, 884-887.	2.6	15
44	Crystal plasticity and hardening: A dislocation dynamics study. Procedia Engineering, 2009, 1, 241-244.	1.2	14
45	High-energy transmission Laue micro-beam X-ray diffraction: a probe for intra-granular lattice orientation and elastic strain in thicker samples. Journal of Synchrotron Radiation, 2012, 19, 307-318.	1.0	14
46	Radiation damage in a micron-sized protein crystal studied via reciprocal space mapping and Bragg coherent diffractive imaging. Structural Dynamics, 2015, 2, 041704.	0.9	14
47	Bragg coherent diffraction imaging and metrics for radiation damage in protein micro-crystallography. Journal of Synchrotron Radiation, 2017, 24, 83-94.	1.0	14
48	Diffraction post-processing of 3D dislocation dynamics simulations for direct comparison with micro-beam Laue experiments. Materials Letters, 2012, 89, 66-69.	1.3	13
49	Analysis of the internal structure and lattice (mis)orientation in individual grains of deformed CP nickel polycrystals by synchrotron X-ray micro-diffraction and microscopy. International Journal of Fatigue, 2012, 42, 1-13.	2.8	13
50	Lifetime of high-order thickness resonances of thin silicon membranes. Ultrasonics, 2015, 56, 116-121.	2.1	13
51	Non-contact, non-destructive mapping of thermal diffusivity and surface acoustic wave speed using transient grating spectroscopy. Review of Scientific Instruments, 2020, 91, 054902.	0.6	13
52	Residual stress characterization in 12%-Cr steel friction stir welds by neutron diffraction. Journal of Strain Analysis for Engineering Design, 2012, 47, 203-213.	1.0	12
53	Simultaneous X-ray diffraction, crystallography and fluorescence mapping using the Maia detector. Acta Materialia, 2018, 144, 1-10.	3.8	12
54	Transient grating spectroscopy of thermal diffusivity degradation in deuterium implanted tungsten. Scripta Materialia, 2020, 174, 6-10.	2.6	12

#	Article	IF	CITATIONS
55	Synchrotron based reciprocal space mapping and dislocation substructure analysis. Materials Letters, 2009, 63, 1077-1081.	1.3	11
56	Digital image correlation and finite element analysis of inter- and intra-granular deformation. Procedia Engineering, 2009, 1, 197-200.	1.2	11
57	Combining Laue Microdiffraction and Digital Image Correlation for Improved Measurements of the Elastic Strain Field with Micrometer Spatial Resolution. Procedia IUTAM, 2012, 4, 133-143.	1.2	11
58	Orientation-dependent indentation response of helium-implanted tungsten. Applied Physics Letters, 2019, 114, 221905.	1.5	11
59	A method for the <i>in situ</i> measurement of evolving elliptical cross-sections in initially cylindrical Taylor impact specimens. Journal of Strain Analysis for Engineering Design, 2010, 45, 429-437.	1.0	10
60	RICH TOMOGRAPHY TECHNIQUES FOR THE ANALYSIS OF MICROSTRUCTURE AND DEFORMATION. International Journal of Computational Methods, 2014, 11, 1343006.	0.8	10
61	3D reconstruction of the spatial distribution of dislocation loops using an automated stereo-imaging approach. Ultramicroscopy, 2018, 195, 58-68.	0.8	10
62	Mapping data between sample and detector conjugated spaces in Bragg coherent diffraction imaging. Journal of Synchrotron Radiation, 2019, 26, 2055-2063.	1.0	10
63	Revealing nano-scale lattice distortions in implanted material with 3D Bragg ptychography. Nature Communications, 2021, 12, 7059.	5.8	10
64	INTRAGRANULAR LATTICE MISORIENTATION MAPPING BY SYNCHROTRON X-RAY MICRO-BEAMS: LAUE VS ENERGY-RESOLVED LAUE VS MONOCHROMATIC RECIPROCAL SPACE ANALYSIS. International Journal of Modern Physics B, 2010, 24, 279-287.	1.0	9
65	Surface terraces in pure tungsten formed by high temperature oxidation. Scripta Materialia, 2019, 173, 110-114.	2.6	9
66	Helium-Ion-Implantation in Tungsten: Progress towards a Coherent Understanding of the Damage Formed and its Effects on Properties. Procedia IUTAM, 2017, 21, 78-85.	1.2	8
67	Probing multi-scale mechanics of peripheral nerve collagen and myelin by X-ray diffraction. Journal of the Mechanical Behavior of Biomedical Materials, 2018, 87, 205-212.	1.5	8
68	Thermal diffusivity recovery and defect annealing kinetics of self-ion implanted tungsten probed by insitu transient grating spectroscopy. Acta Materialia, 2022, 232, 117926.	3.8	8
69	Orientation dependence of the nano-indentation behaviour of pure Tungsten. Scripta Materialia, 2020, 189, 135-139.	2.6	7
70	Estimate for thermal diffusivity in highly irradiated tungsten using molecular dynamics simulation. Physical Review Materials, 2021, 5, .	0.9	7
71	Intrinsic to extrinsic phonon lifetime transition in a GaAs–AlAs superlattice. Journal of Physics Condensed Matter, 2013, 25, 295401.	0.7	6
72	Annealing of focused ion beam damage in gold microcrystals: an <i>in situ</i> Bragg coherent X-ray diffraction imaging study. Journal of Synchrotron Radiation, 2021, 28, 550-565.	1.0	6

#	Article	IF	CITATIONS
73	Probing Deformation Substructure by Synchrotron X-ray Diffraction and Dislocation Dynamics Modelling. Journal of Nanoscience and Nanotechnology, 2010, 10, 5935-5950.	0.9	5
74	ON THE MEASUREMENT AND INTERPRETATION OF RESIDUAL STRESS AT THE MICRO-SCALE. International Journal of Modern Physics B, 2010, 24, 1-9.	1.0	5
75	Observation of crack growth in a polycrystalline ferroelectric by synchrotron X-ray diffraction. Scripta Materialia, 2017, 140, 23-26.	2.6	5
76	New perspectives on collision cascade damage in self-ion irradiated tungsten from HR-EBSD and ECCI. Journal of Nuclear Materials, 2021, 554, 153074.	1.3	5
77	Eigenstrain analysis of non-uniformly shaped shot-peened samples. Procedia Engineering, 2009, 1, 151-154.	1.2	4
78	Residual stress measurement on the I12 JEEP beamline at Diamond Light Source. Diamond Light Source Proceedings, 2010, 1, .	0.1	4
79	Mapping of domain structure in Barium Titanate single crystals by synchrotron x-ray topography. Proceedings of SPIE, 2010, , .	0.8	4
80	Polycrystalline materials analysis using the Maia pixelated energy-dispersive X-ray area detector. Powder Diffraction, 2017, 32, S16-S21.	0.4	4
81	Synchrotron X-ray analysis of microstructure and microdeformation in a recast AA6063 aluminium alloy. Journal of Strain Analysis for Engineering Design, 2010, 45, 351-364.	1.0	3
82	Measurements of Long-range Electronic Correlations During Femtosecond Diffraction Experiments Performed on Nanocrystals of Buckminsterfullerene. Journal of Visualized Experiments, 2017, , .	0.2	3
83	Synchrotron investigations of non-uniformly shaped shot-peened samples. Zeitschrift Für Kristallographie, Supplement, 2009, 2009, 315-320.	0.5	3
84	Deformation behaviour of ion-irradiated FeCr: A nanoindentation study. Journal of Materials Research, 2022, 37, 2045-2060.	1.2	2
85	Shedding coherent light on defects. Nature Materials, 2015, 14, 756-757.	13.3	1
86	Multi-modal Nanoscale Imaging of Materials and Biology. Microscopy and Microanalysis, 2018, 24, 32-33.	0.2	1
87	In situ Bragg coherent X-ray diffraction imaging of corrosion in a Co–Fe alloy microcrystal. CrystEngComm, 0, , .	1.3	1
88	Micro-scale characterization of deformation and distortion in ductile (poly)crystals by synchrotron X-ray beams. Diamond Light Source Proceedings, 2010, 1, .	0.1	0
89	Combined micro-beam Laue and white beam topography: mapping local lattice orientation and misorientation. Diamond Light Source Proceedings, 2010, 1, .	0.1	0
90	Probing mesoscopic lattice misorientation by strain gradient crystal plasticity modelling and micro-beam Laue diffraction experiments. International Journal of Theoretical and Applied Multiscale Mechanics, 2011, 2, 12.	0.5	0

#	Article	lF	CITATIONS
91	High-Energy Transmission Laue (HETL) Micro-Beam Diffraction. , 2014, , 82-124.		0
92	Understanding Strain And Irradiation Segregation In Fusion Materials. Microscopy and Microanalysis, 2021, 27, 2648-2649.	0.2	0
93	Computation of Burgers vectors from elastic strain and lattice rotation data. Proceedings of the Royal Society A: Mathematical, Physical and Engineering Sciences, 2022, 478, .	1.0	Ο